FRACTAL STRUCTURE OF SOLAR SUPERGRANULATION

U. Paniveni[1], V.Krishan[1], Jagdev Singh[1], and R. Srikanth[2]

[1]Indian Institute of Astrophysics, Koramangala,Bangalore-34, India
[2]Raman Research Institute, Sadashivanagar, Bangalore-80, India

ABSTRACT

We employ fractal analysis to study the complexity of supergranulation structure using the Solar and Heliospheric Observatory (SOHO) dopplergrams. Our data consists of 200 visually selected supergranular cells, for which we find a broad, slightly asymmetric dispersion in the size distribution, with the most probable size around 31.9 Mm. From the area-perimeter relation, we deduce a fractal dimension D of about 1.25. This is consistent with that for isobars, and suggests a possible turbulent origin of supergranulation. By relating this to the variances of kinetic energy, temperature and pressure, it is concluded that the supergranular network is close to being isobaric and that it has a possible turbulent origin.

Key words: Solar supergranulation; fractal structure.

1. INTRODUCTION

High resolution observations of the solar photosphere have long indicated that the solar surface is granular and shows irregular polygonal brightness patterns surrounded by dark lanes. These cellular velocity patterns are a visible manifestation of the sub-photospheric convection currents which contribute substantially to the outward transport of energy from the deeper layers, thus maintaining the energy balance of the Sun as a whole.

The solar convection zone, of thickness equal to 30% of the solar radius, lies below the photosphere and is revealed by two surface network patterns. On the scale of 1000 km it is the granulation, with a typical lifetime of 8-10 min and on a scale of 30000 km, it is supergranulation with a typical lifetime of 24 hr. Supergranules are observed in the high photosphere as large convective eddies with horizontal diverging flows from the cell centre and subsiding flows at the cell borders. Horizontal currents associated with each supergranule are believed to sweep magnetic fields from the declining active regions into the boundaries of the cell where they produce excess heating resulting in the chromospheric network.

A dependence of the network size on the magnetic activity has been suggested (Chandrashekar 1961). Sykora (1970) and Raju et al. (1998) report a dependence of cell size on solar latitude. Berrilli et al. (1999) find a 2% anisotropy for the chromospheric network cell orientation and a 30% size reduction towards the poles. Lisle et al. (2004) have noted a north-south alignment of supergranulation, consistent with an underlying dynamical cause at a larger scale, identified with giant cells. Similarly a dependence of the calcium network cell size on the solar cycle, with a smaller size at solar maxima, has been reported by Singh and Bappu (1981). Singh et al. (1994) have also reported a positive correlation between cell sizes and cell lifetimes.

The bright chromospheric network observed in Ca II K and Hα core filtergrams shows a dependence of autocorrelation size of the cells on the latitude. The size shows an approximate N-S symmetry with two minima at 20° N and 20° S (Raju, Srikanth and Singh 1998). Active cells close to the periphery of a plage are found to live longer than those in the quiescent regions. The confining properties of the magnetic field may be responsible for the longer life of active cells.

Srikanth et al. (1999) have also found a positive correlation between cell sizes and cell lifetimes. Diffusion-like dispersion of the magnetic flux is the dominant factor in the large-scale evolution of the network. Convective motion and magnetic inhibition of the motion are both stronger in active regions, thereby leading to similar speeds in all regimes (Srikanth, Singh and Raju 1999). A relationship between horizontal flow velocity and the size of a supergranular cell has been established by Krishan et al. (2002). The corresponding dependence of the lifetime T of the supergranular cell on its horizontal flow velocity is found to be $v_h \propto T^{0.5}$. Here T, also the eddy turnover time is estimated from the relation $T = L/v_h$ with L as the distance from the centre to the edge of the cell (Paniveni et. al 2004).

Fractal analysis is a valuable mathematical tool to quantify the complexity of geometric structures and thus gain insight into the underlying dynamics. For example, statistical analyses like studies of the size distribution of ac-

Proceedings of the 11th European Solar Physics Meeting - The Dynamic Sun: Challenges for Theory and Observations, 11-16 September 2005 (ESA SP-596, December 2005)

tive regions or of the fractal dimension of solar surface magnetic fields in the photosphere are useful for comparing observations and models. They can shed light on the turbulence of the magnetoconvective processes that generate the magnetic structures (Stenflo, Holzreuter 2003a; Lawrence, Ruzmaikin, Cadavid 1993).

For our purpose, the fractal dimension D is characterized by the area-perimeter relation of the structures (Mandelbrot 1977). Self-similarity, or geometric scale-invariance, is expressed by a linear relationship between $\log P$ and $\log A$ (Eq. 1) over some range of scales.

Fractal analysis was first applied to a solar surface phenomena by Roudier and Muller (1987), who measured the fractal dimension of granular perimeters. From Pic du Midi data, they find a fractal dimension $D = 1.25$ for granular diameters of size $d \leq 1''.37$ and $D \approx 2$ for larger granules.

2. DATA ANALYSIS

We analysed 33 hour data of full disc Dopplergrams obtained on 28th and 29th June 1996 by the Michelson Doppler Interferometer (MDI) on board the Solar and Heliospheric observatory (SOHO) (Scherrer et al. 1995).

The SOHO full disc dopplergram data has been obtained with a resolution of $2''$ which is twice the granular scale. Further, the dopplergrams are time averaged over intervals of 10 min, which is about twice the 5-minute period of oscillations. Thus the signal due to granular velocity is averaged out. Similarly the contributions due to p-mode vibrations are reduced after the time averaging. Our analysis rests on the implicit belief that time averaging removes noise significantly, as judged from visual inspection and also as seen in typical supergranular velocity profile for our data (cf.Fig. 1 of Paniveni et al.(2004)). After the averaging, the supergranular network is brought out with a fair clarity. This procedure yielded usually six images per hour of the data. Corrections due to solar rotation are applied to the dopplershifts. Two hundred well accentuated cells lying between 15° and 60° angular distance from the disc centre were selected. Restricting to the above mentioned angular distance limits helps us discount weak supergranular flows as well as foreshortening effects. A previous study (Srikanth 1999) noted a possible tendency for smaller supergranules to have smoother, less corrugated boundaries than larger supergranules, which was attributed to the weakening of the supergranular outflow pressure with radial distance. Nevertheless, we believe any such bias is minimal in our study as all length-scales seem to be well represented, as seen in Table 1.

3. SUPERGRANULAR CELL AREA AND PERIMETER

The profile of a visually identified cell was scanned as follows: we chose a fiducial y-direction on the cell and performed velocity profile scans along the x-direction for all the pixel positions on the y-axis. In each scan, the cell extent is taken to be marked by two juxtaposed 'crests' (separated by a 'trough'), expected in the dopplergrams. This set of data points was used to determine the area and perimeter of a given cell, and of the spectrum for all selected supergranules. The area-perimeter relation is used to evaluate the fractal dimension.

4. RESULTS AND DISCUSSION

The main results pertaining to the maximum, minimum, mean, standard deviation and the skewness for cell area A and cell perimeter P are summarized in Table 1. A large dispersion in the area and perimeter was obtained. The area distribution (Figure 1) shows an asymmetry, with a steeper rise on the smaller scale and gentler fall on the larger scale. It peaks at a characteristic size of around 8×10^8 km^2, or a diameter 31.9 Mm assuming circularity.

We analyzed planar shapes by analyzing the area-perimeter relation,

$$P \propto A^{D/2} \tag{1}$$

The $\log(A)$ vs $\log(P)$ relation is linear as shown in the lower frame of Figure (2). A correlation co-efficient of 0.92 indicates strong correlation. Fractal dimension D, calculated as (2/slope), is found to be $D = 1.345\pm0.082$. If we interchange the $\log(A)$ and $\log(P)$ axes (upper frame, Figure 2), fractal dimension D here is 2 $\times$ slope and found to be $D = 1.136 \pm 0.070$. The small difference in D values thus obtained may be because error bars in P and A are not symmetric. The average over the two methods is $D = 1.24 \pm 0.076$. For smooth shapes such as circles and squares $P \propto A^{1/2}$ and thus $D = 1$, the dimension of a line. As the perimeter becomes more and more contorted and tends to double back on itself filling the plane, so that $P \propto A$ and D approaches the value 2, a maximum. The linear relation (Figure 2) suggests that supergranules are self-similar and may be regarded as fractal objects. Unlike the case of granules, we do not find any multifractal structure. So it seems likely that the entire distribution profile can be explained by a single physical phenomenon. Since $P \propto A^{D/2}$, we may expect D to be an important parameter characterizing the processes which poduces the solar supergranulation.

The spectral distribution of the temperature, a passive scalar, is related to the spectral distribution of kinetic energy. It can be easily shown that the Kolmogorov energy spectrum , $K^{-5/3}$, both in two and three dimensional turbulence leads to a temperature spectrum of

$K^{-5/3}$ (Krishan 1991; 1996). Thus the temperature variance $\langle\theta^2\rangle$ varies as $r^{2/3}$, as a function of the distance r (Tennekes and Lumley 1970). According to Mandelbrot (1975), an isosurface has a fractal dimension given by D_I = (Euclidean dimension) - 1/2 (exponent of the variance). Thus for two dimensional supergranulation $D_T = 2 - (1/2 \times 2/3) = 5/3 = 1.66$ for an isotherm. The pressure variance $\langle p^2\rangle$ on the other hand is proportional to the square of the velocity variance i.e. $\langle p^2\rangle \propto r^{4/3}$ (Batchelor 1953). The fractal dimension of an isobar is, therefore, found to be $D_p = 2 - (1/2 \times 4/3) = 1.33$. Our data furnishes a fractal dimension $D = 1.25$ which indicates that the supergranular network is close to being an isobar. It is interesting to note that Roudier and Muller (1987) obtained a similar dimension for smaller granules.

To characterize the shape of the distributions for the area and perimeter, we computed skewness and kurtosis. Skewness is a measure of the extent of departure from the symmetry of the distribution about the mean. It is positive here indicating that cell area and perimeter values are bunched at lower values than the mean. The error on this statistic is computed as $\sqrt{6/N}$ (Brown 1996), where $N = 200$ is the number of cells. The respective values for cell area and perimeter are given in Table 1. Kurtosis is a measure of the peakedness of the distribution about the mean, with a normal distribution represented by zero kurtosis. We obtain a kurtosis value of 0.109 for the area and 0.474 for the perimeter distributions. For our data, the standard error in kurtosis is given by $\sqrt{24/N} = 0.346$. Since twice this value is larger than the absolute values we obtain for area and perimeter kurtosis, we conclude that the values we have obtained are within the expected range of chance fluctuations and hence insignificant for our sample size and binning we have chosen (Brown 1996). The standard error on standard deviation is computed as $\sigma/\sqrt{N}$.

The value of the fractal dimension derived from the Dopplergram compares well with that derived from the Ca K intensity data. It should be instructive to explore the relative merits and results of the different data sets such as Dopplergrams, magnetograms and intensity patterns for a better understanding of the solar convective phenomena.

ACKNOWLEDGEMENT

We thank Dr. P. H. Scherrer and the SOHO consortium for providing us with the MDI/SOI data.

REFERENCES

[1] Batchelor, G.K., *The theory of Homogeneous Turbulence* (Cambridge University Press 1953)

[2] Berrilli, F., Ermolli, I., Florio, A., Pietropaolo, E., A&A 344, 965 (1999).

[3] Brown, J. D., *Testing in language programs* (Upper Saddle River, NJ: Prentice Hall, 1996).

[4] Chandrasekhar,S. : *Hydrodynamic and Hydromagnetic Stability* (Clarendon Press, Oxford 1961).

[5] Krishan,V.,1991, MNRAS, 250, 50

[6] Krishan,V.,1996 Bull.Astrom.Soc.India, 24, 285.

[7] Krishan,V., Paniveni,U., Singh,J., Srikanth,R., 2002, MNRAS, 334/1, 230

[8] Lawrence, J. K., Ruzmaikin, A. A., Cadavid, A. C. Astrophysical Journal v.417, p.805 (1993).

[9] Lisle, Jason P., Rast, M. P.; Toomre, J., ApJ, 608, 1167 (2004).

[10] Mandelbrot, B. 1977, Fractals (San Francisco: Freeman)

[11] Benoit,B. Mandelbrot , 1975, J.Fluid Mech.,72, part2, pp. 401-416
308, 213

[12] Paniveni, U., Krishan, V., Singh, J., Srikanth, R., 2004, MNRAS, 347,1279-1281

[13] Raju,K.P., Srikanth,R. and Jagdev Singh: 1998, Solar Physics, 180, 47.

[14] Roudier,Th. and Muller, R., 1986, Solar Physics, 107, 11.

[15] Scherrer, P. H., et al., 1995, Solar Physics, 162, 129.

[16] Singh,J. and Bappu, M. K. V., 1981, Solar Physics, 71, 161.

[17] Singh,J., Nagabhushana,B. S., Babu,G. S. D. and Wahab Uddin, 1994, Solar Physics, 153, 157

[18] Srikanth, R., 1999, Chapter 3, PhD thesis, Indian Institute of Science.

[19] Srikanth, R., Singh, J. and Raju, K. P., 1999, Solar Physics, 187, 1.

[20] Srikanth, R., Raju, K. P. and Singh, J., 1999, Solar Physics, 184, 267

[21] Stenflo, J. O., and Holzreuter, R. in Current Theoretical Models and Future High Resolution Solar Observations: Preparing for ATST, ed. A. A. Pevtsov, & H. Uitenbroek, ASP Conf. Ser., 286, 169 (2003a).

[22] Sykora, J., 1970, Solar Physics, 71, 161

[23] Tennekes, H. and Lumley, J.L. *A First course in Turbulence* (MIT press 1970)

	Max	Min	Mean	σ	skewness
A (Mm^2)	912.4	97.0	375.3	152.8 ± 10.8	0.74 ± 0.17
P (Mm)	169.3	41.6	89.3	23.5 ± 1.7	0.83 ± 0.17

Table 1. Maximum, minimum, mean, standard deviation and skewness for area (A) and Perimeter (P).

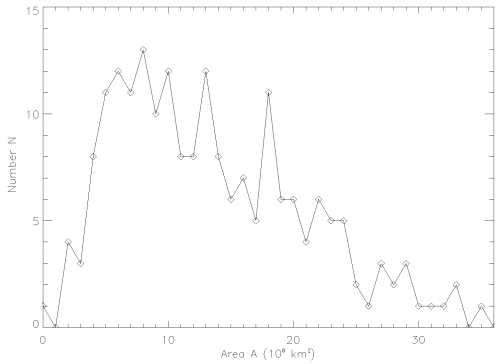

Figure 1. Histogram of Area A in $10^8 km^2$ against number N of the cells.

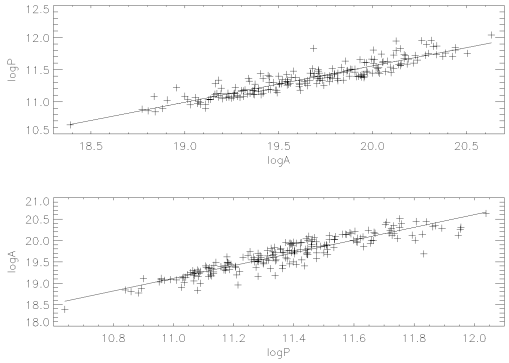

Figure 2. Plot of the natural logarithm of the supergranular area (in km^2) against the natural logarithm of perimeter (in km) in the lower frame; and ordinate and coordinate axes are interchanged in the upper frame.